IN-SITU NEUTRON DIFFRACTION STUDY OF AGING OF A Mg-Y-Nd-Zr ALLOY (WE43): EFFECTS OF PRECIPITATION ON INDIVIDUAL DEFORMATION MECHANISMS

S.R. Agnew,[1] F.J. Polesak, III,[1] and B. Clausen[2]

[1]Materials Science and Engineering, University of Virginia;
Charlottesville; VA; 22904-4745 U.S.A.
[2]Materials Science and Technology Division, Los Alamos National Laboratory;
Los Alamos; NM; 87454 U.S.A.

Keywords: precipitation, aging, basal, non-basal, twinning, neutron diffraction, internal stress

Abstract

There is an outstanding question regarding why the age hardening response of Mg alloys is not nearly as good as many competing Al alloys. It has recently been proposed that the effect is due to precipitate geometry, since most commercial Mg alloys form either basal plate-shaped precipitates (e.g. AZ alloys) or c-axis aligned rod-shaped precipitates (e.g. ZK alloys) [1], and these are among the least effective precipitate shapes to obstruct basal slip. It is further proposed that prismatic plate-shaped precipitates would be most effective for strengthening Mg alloys [1], and prior transmission electron microscopy studies have revealed that Mg-Y-Nd-Zr alloys form prismatic plate shaped precipitates during artificial aging. In-situ neutron diffraction experiments performed on Mg-Y-Nd-Zr alloy, WE43, in the solution heat treated and peak- and over-aged conditions, reveal that prismatic plate shaped precipitates do indeed strongly impede basal slip. However, as revealed by previous in-situ neutron diffraction and crystal plasticity studies of Mg alloys, hard deformation modes such as deformation twinning and non-basal slip are required for macroscopic yielding. These hard modes are not as strongly impeded by the prismatic plate shaped precipitates. This finding helps to explain why the age hardening response of Mg-Y-Nd-Zr alloys is not that great, and suggests that the main reason these alloys are so strong relates to potent solid solution strengthening, in addition to precipitation strengthening. It is concluded that the future alloy and process design strategies should focus on promoting high number densities of particles more than on particle shape.

Introduction

It has recently been suggested [1] that the basal plates typical of Mg-Al alloys [1] and c-axis rods typical of Mg-Zn [1] are among the least effective types of precipitate morphologies for strengthening hexagonal close packed metals, which deform primarily by basal slip. In contrast, prismatic plates are proposed to be the most effective strengthening morphology [1] for such a material. In support of this theoretical work is the empirical fact that some of the highest strength Mg alloys are Mg-Y-RE (rare earth) alloys, where it has been shown that prismatic plate-shaped precipitates can be formed, particularly in alloys of the Mg-Y-Nd system [1]. What is missing from these precipitation hardening analyses is an admission that non-basal slip and twinning play a critical role in determining the yield strength and strain hardening behavior of Mg alloys. In situ neutron diffraction and crystal plasticity modeling studies, in particular, have illustrated that hard deformation mechanisms play a major role in determining the macroscopic yield strength of wrought Mg alloys, AZ31 [e.g.1,2] and ZM20 [1,2].

In situ neutron diffraction has actively been used to explore the distribution of slip and twinning in Mg alloys. One of the fist in situ neutron diffraction work on this problem was led by Gharghouri [1], who showed that twinning is primarily controlled by Schmid stresses, and that large, blocky precipitates in a Mg-Al alloy impeded twinning more than they do slip (i.e., the tension-compression

Report Documentation Page	*Form Approved* *OMB No. 0704-0188*

1. REPORT DATE **JUL 2012**	2. REPORT TYPE	3. DATES COVERED **00-00-2012 to 00-00-2012**

4. TITLE AND SUBTITLE **In-SITU Neutron Diffraction Study Of Aging Of A Mg-Y-Nd-Zr Alloy (WE43): Effects Of Precipitation On Individual Deformation Mechanisms**	5a. CONTRACT NUMBER
	5b. GRANT NUMBER
	5c. PROGRAM ELEMENT NUMBER
6. AUTHOR(S)	5d. PROJECT NUMBER
	5e. TASK NUMBER
	5f. WORK UNIT NUMBER
7. PERFORMING ORGANIZATION NAME(S) AND ADDRESS(ES) **University of Virginia,Materials Science and Engineering,Charlottesville,VA,22904**	8. PERFORMING ORGANIZATION REPORT NUMBER
9. SPONSORING/MONITORING AGENCY NAME(S) AND ADDRESS(ES)	10. SPONSOR/MONITOR'S ACRONYM(S)
	11. SPONSOR/MONITOR'S REPORT NUMBER(S)

12. DISTRIBUTION/AVAILABILITY STATEMENT
Approved for public release; distribution unlimited

13. SUPPLEMENTARY NOTES
Presented at Mg2012: 9th International Conference on Magnesium Alloys and their Applications, Vancouver, BC, Canada, July 8-12, 2012, Government or Federal Purpose Rights License

14. ABSTRACT

15. SUBJECT TERMS

16. SECURITY CLASSIFICATION OF:			17. LIMITATION OF ABSTRACT	18. NUMBER OF PAGES	19a. NAME OF RESPONSIBLE PERSON
a. REPORT **unclassified**	b. ABSTRACT **unclassified**	c. THIS PAGE **unclassified**	**Same as Report (SAR)**	**9**	

asymmetry of textured polycrystals diminishes.) This latter result is in agreement with early work of Clark [2], and has also been validated by recent studies of a Mg-Al alloy by Jain et al. [1]. However, this result is distinct from Clark's earlier results obtained from samples of Mg-5wt%Zn, which showed that twinning is not strongly impeded by the Mg-Zn precipitates [2]. A major difference between the two alloying systems is that precipitation in the Mg-Zn system results in finer, well-distributed rod-shaped particles aligned with the c-axis rather than the basal plates or large, blocky particles found in the Mg-Al system. Recent results obtained with collaborators Wu et al. [1] on alloy ZK60 have confirmed that twinning is not strongly impeded by the fine precipitates in the Mg-Zn system. In fact, a very recent study has shown that such fine precipitates may actually promote twin nucleation [1,2].

The present study seeks to answer the outstanding questions about the effect of precipitation on slip and twinning in magnesium alloys (e.g., does a prismatic plate precipitate morphology much more strongly affect the critical resolved shear strength of basal slip than it does prismatic slip?) In situ neutron diffraction was performed on the Mg-Y-Nd-Zr alloy, WE43, in three different conditions (solutionized, peak- and over-aged) with distinct precipitate microstructures.

Experimental Procedure

The material was direct-chill cast by Magnesium Elektron UK in Swinton, Manchester, England. A block from the cast slab was provided for the present experiments. Smaller sections were cut from the block and solution heat treated at 525°C for 8 hours and quenched in water. The initial microstructure of the as-cast and solutionized conditions is shown below (Fig. 1). While the eutectic was fully dissolved by the homogenization treatment, the Zr rich "pips" within the grains did not dissolve, nor did Y-rich cuboidal phases that appeared at the edges of the eutectic region in the casting [1]. One sample was then peak aged for 16 hours at 250ºC followed by air cooling, per industrial practice [1], and another sample was over-aged, 793 hours (33 days). The Vickers hardness was measured 15 times on a ground and polished section of each sample. The results are shown below in Fig. 1, right. While the solutionized sample was the softest, the age hardening response is not that significant (only an increase of about 10 on the Vickers hardness scale). Further, the results suggest that the "peak-aged" condition is simply an optimization of the property and time in the furnace required to obtain it, since the "over-aged" sample is actual harder. The alloy clearly resists degradation of the strength at temperatures up to 250ºC for intermediate exposure times of order one month.

Pole figures of the initial texture were obtained using the Schulz reflection method in a Scintag X1 X-ray diffractometer equipped with a CuK_{α} sealed tube source, an energy dispersive detector, and a 4-circle goniometer. The (00.1), (10.0), and (10.1) pole figures were measured and the preferred orientation package of Los Alamos (popLA) software was used to calculate the complete orientation distribution which, in turn, allowed the recalculation and presentation of complete pole figures. The pole figures (not shown here in the interest of space) reveal that the texture is essentially random. There are a number of isolated peaks with intensities of approximately 2 multiples of a random distribution, but these spotty features are associated with the coarse grain structure and not indicative of any significant preferred orientation.

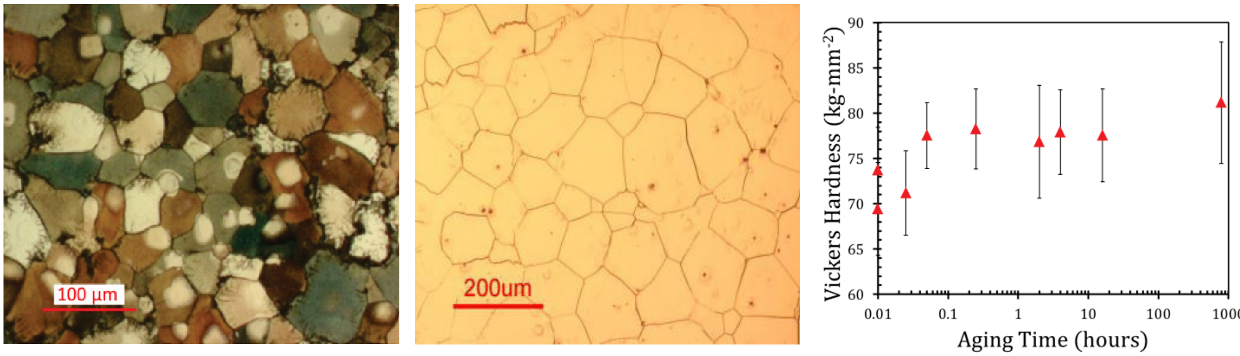

Figure 1. Microstructure of alloy WE43 in the as-cast (left) and solutionized (middle) conditions. The microhardness as a function of aging at 250ºC is shown at right.

Compression samples were electrical discharge machined from the small blocks. The solutionized and over-aged compression samples had nominal diameters of 8mm and nominal lengths of 20mm (a 2.5:1 length-to-diameter ratio). The peak-aged sample had a nominal diameter of 6mm and a nominal length of 14mm (a 2.33:1 length-to-diameter ratio). The neutron diffraction measurements were performed on the Spectrometer for Materials Research at Temperature and Stress (SMARTS) at the Manuel Lujan Jr. Neutron Scattering Center, a part of Los Alamos Neutron Science Center (LANSCE), at Los Alamos National Laboratory. Details of the instrument are published elsewhere, [1] so only a short description is presented here. The compression sample is horizontally loaded in the custom Instron load frame with a 45° orientation relative to the incident neutron beam (see Fig. 1 of ref. [2]). The samples must be pre-loaded to 5 MPa to keep them in the horizontal grips. An extensometer was attached to the irradiated region to measure the macroscopic strain. Two ^{3}He detector banks are positioned ±90° relative to the incident beam, allowing for collection of diffraction patterns corresponding to lattice strains both parallel (-90°) and perpendicular (+90°) to the applied load. The samples were loaded and then held at a constant position while the diffraction measurements were acquired. Internal strains within grains that satisfy the Bragg condition for a given (hkl) reflection are calculated from the difference between the measured and initial lattice spacing:

$$\varepsilon = \frac{d - d_0}{d_0}, \tag{1}$$

where d is the measured lattice spacing and d_0 is the initial stress-free lattice spacing. Lattice spacing and subsequent internal strain calculations were determined by single peak fits using an instrument specific code developed at LANSCE (e.g. SMARTSreflist and SMARTSmacro codes were used for further data analysis on each sample). The former code extracts the mean random distribution intensity data from Rietveld refinements and the latter makes time averages of the load frame data for each run.

Results

The macro stress-strain curves illustrate the mechanical behavior of the solutionized, peak- and over-aged materials (Fig. 2). The solutionized sample exhibits microyielding at a rather low stress of approximately 60 MPa, followed by rapid strain hardening. The peak- and over-aged samples do not show such protracted microyielding. Rather, they undergo a more sudden elastoplastic transition at approximately 150 MPa. Beyond the elastoplastic transition, all of the samples strain harden at a very similar rate. The curvature in the unload curves shows that all of the samples exhibit pseudoelastic effect recently highlighted by Caceres et al. [2] and further studied by in-situ neutron diffraction by Muransky et al. [2]. Finally, the stress drops along the curves are artifacts of the in-situ testing method, they are not indicative of a material effect such as serrated flow. Rather,

the samples are held at a constant strain for 20 minutes or so, while the neutron diffraction data is being collected. During this time, some stress relaxation occurs. The data points indicate the time average stress and strain values during these hold periods and correlate with internal strain data points shown in below.

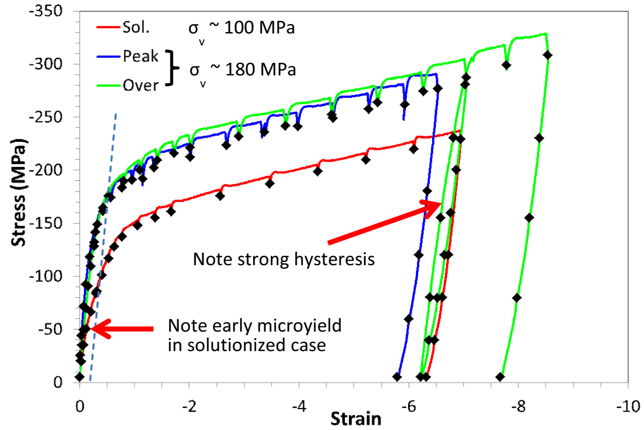

Figure 2. Compressive stress strain curves reveal a distinction in the elastoplastic transition of solutionized and that of the peak- and over-aged samples, respectively. The solutionized material microyields at a low stress and rapidly strain hardens before reaching the lower strain hardening rate more immediately adopted by the peak- and over-aged samples.

The internal strains within sets of grains parsed by their orientation by the Bragg diffraction condition are plotted as a function of the applied macroscopic flows stress in Fig. 3. The internal strain evolution with applied stress includes various inflection points which can be attributed to the activation of various deformation mechanisms. When the internal strain of a given set of grain orientations diverges vertically, that is indication that the particular set of grains represents "soft orientations." Such grains have begun accommodating plastic strain and decreasing the amount of elastic loading. When this occurs, the "harder oriented" sets of grains simultaneously begin accommodating more elastic load, causing a divergence to the right. The average response cannot deviate from Hooke's law, indicated by the solid black like in each of the plots below.

These results show that all grain orientations strain quite similarly until the point of micro-yielding, where the first inflection can be seen. This similarity in grain-level lattice strains (or elastic stresses) is a result of the near elastic isotropy exhibited by Mg and its alloys. The first inflection has been associated with the activation of basal slip [e.g.5]. Notably, this inflection occurs at a much lower stress in the solutionized material (Fig. 2, top) than the other two (Figs. 2 middle and bottom), consistent with its lower microyield stress seen in the macro flow curves (Fig. 1). A second inflection point can be seen at higher stress levels, which correspond to the activation of deformation twinning and/or non-basal slip of <a> type dislocations. In the solutionized sample, there is about 80 MPa between the activation of basal slip and twinning, but in the peak-aged and over-aged samples, there is only about 40 MPa.

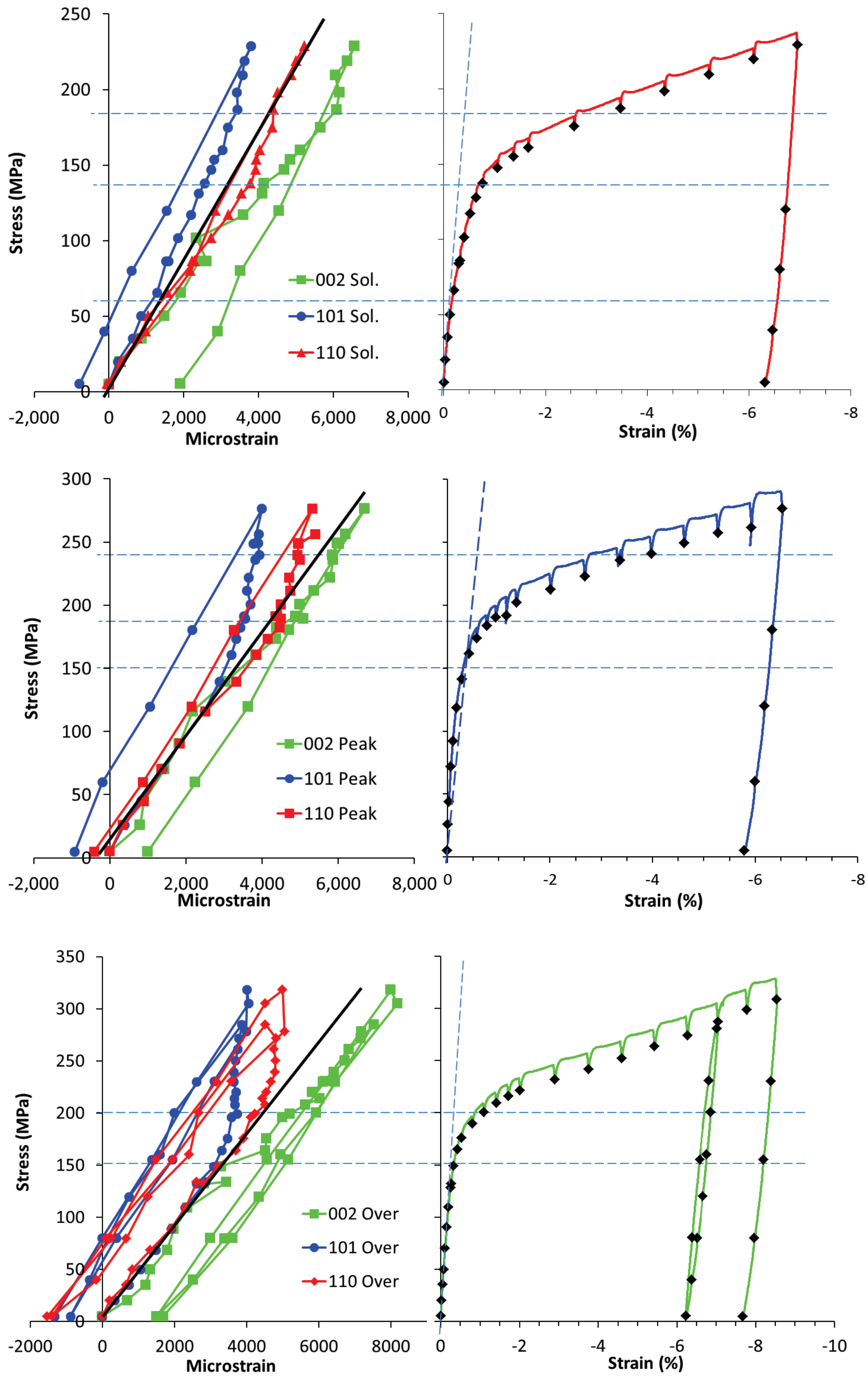

Figure 3. Internal stresses (i.e. microstrain) measured by in-situ diffraction and presented as a function applied stress for samples in the solutionized (top), peak- (middle) and over-aged (bottom) conditions.

As shown in the macroscopic stress strain curve, the first inflection in the internal strains determined by in-situ neutron diffraction data show that the solutionized WE43 microyields ~60 MPa. This inflection is most obvious in the {10.1} oriented grains, which are soft oriented with respect to basal slip, i.e. the Schmid factor, m ~ 0.46. The second inflection, most obvious in the {11.0} grains, occurs at ~140 MPa. These grains are soft oriented with respect to prism slip/twinning, m ~ 0.37. In contrast, the inflection in the {10.1} oriented grains within the peak-aged WE43 sample does not occur until ~150MPa. This suggests an increase in the longitudinal critical stress to initiate basal slip of ~90 MPa. However, second inflection, which is most obvious in the {11.0} grains, occurs at ~190 MPa. This is only ~50 MPa higher than solutionized condition. Similar to the peak-aged sample, the over-aged WE43 also microyields ~150MPa, as indicated by the vertical departure of the internal strains within the {10.1} grains from the aggregate response. The second inflection I the internal strain data occurs at ~200 MPa, where the {11.0} oriented grains begin accumulating less internal strain. In summary, the grains well-oriented for basal slip are greatly strengthened by the aging treatment, whereas the grains well-oriented only for hard deformation mechanisms of twinning or prismatic slip are not so greatly strengthened. Deformation twinning leads to a marked evolution in the crystallographic texture, which is readily assessed by the in-situ neutron diffraction measurement. In the present case, the initially randomly textured material adopts a fiber texture with {00.2} poles oriented parallel to the compression axis. Fiber textures can often be well-described by the March-Dollase function:

$$MD\left(r,\alpha\right)=\left(r^2\cos^2\alpha+\frac{\sin^2\alpha}{r}\right)^{-\frac{3}{2}},0<r\le 1 \tag{2}$$

where α is the angle from the compression axis and r is a measure of the fiber texture strength. Here, we simply present the intensity of the fiber texture in multiples of a random distribution as a function of applied stress or strain (Fig. 4). If one considers the degree of texture evolution (indicative of twinning activity) as a function of strain, it appears that precipitation actually promotes twinning. The aged samples show a more rapid texture evolution than the solutionized. On the other hand, presenting the same data as a function of stress shows that aging delays twinning to higher stress levels 175 vs. 140 MPa. It still remains to be determined whether the higher level of twinning in aged WE43 is simply due to the higher stress levels or due to more nuclei that might form in association with the precipitates [12,13].

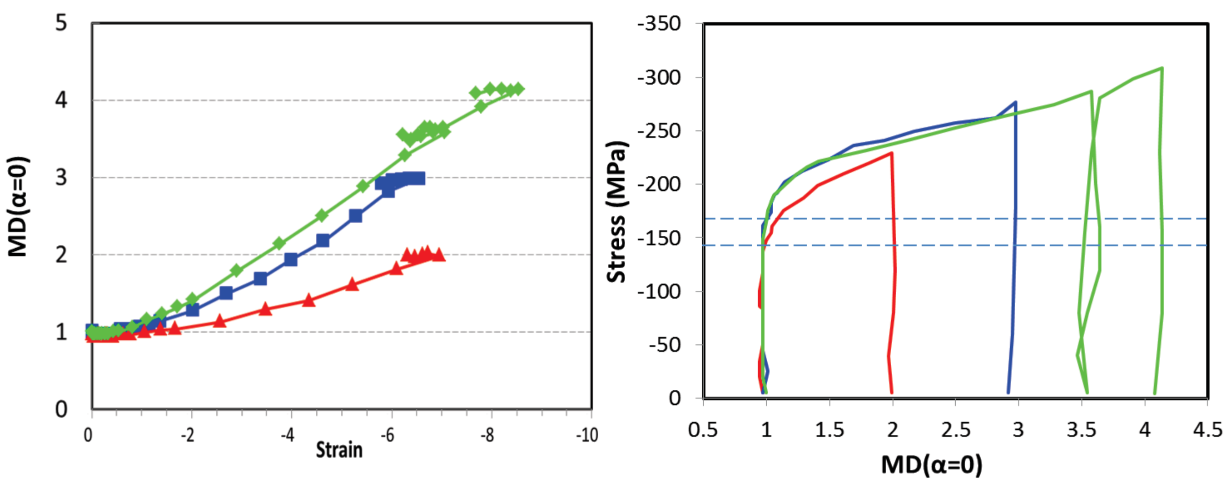

Figure 4. Texture evolution associated with deformation twinning within solutionize, peak- and over-aged samples as a function of strain (left) and stress (right). The reason for switch the abscissa and ordinate are to ease comparison between these plots and Figures 2 and 3.

A summary of the semi-quantitative findings of this experimental study are presented in Table I. It shows that the basal slip mode is strengthened over the solutionized state by the presence of prismatic shaped plates in the peak- and over-aged conditions, by about 90 MPa in axial stress. This translates into ~40 MPa increase in the critical resolved shear strength (CRSS), assuming Schmid law holds via a lower bound estimate of uniform stress throughout the aggregate. Notably, a recent estimate for the increase in the CRSS values due to aging of alloy AZ91 is only 5 MPa [2]. Thus, Nie's hypothesis that basal slip would be much more potently strengthened by the prismatic-shaped plates in WE-alloys appears to be correct. However, the increase in the CRSS corresponding to the activation of either prismatic slip or {10.2} extension twinning is modest, about 20-25 MPa. This is comparable with estimates performed for alloys AZ91 [20]. The offset yield strength better correlates with the activation of the hard deformation modes than it does with the activation of basal slip. Thus, the failure of the precipitates to markedly increase the CRSS of the hard modes helps to explain why the overall aging response of alloy WE43 is modest, despite the fact that basal slip is potently strengthened.

Table I. Summary of experimental results, including the stresses (in MPa) at inflection points and the approximate critical resolved shear strengths of soft and hard modes, assuming a lower bound approximation, and comparison with literature values estimated for alloy AZ91 [20].

	Microyield/ 1^{st} inflect.	***τ(basal) ~ 0.46*σ***	***0.2% Offset yield***	***2^{nd} inflect {11.0}***	***τ(tw/pr) ~ 0.37/0.46*σ***	***Twin initiation***
Solutionized	60	**30**	100	140	**50 / 65**	140
Peak Aged	150	**70**	180	190	**70 / 85**	175
Over Aged	150	**70**	180	200	**75 / 90**	175
Δτ	-	**40**	-	-	**20-25**	-
Δτ(AZ91)	-	**5**	-	-	**20-25**	-

Conclusions

Prismatic plate shaped precipitates typical of Mg-Y-Nd-Zr alloys like WE43 strongly impede basal slip, as indicated by the large increase, with aging, in the stress at which grains well-oriented for basal slip begin accommodating plasticity. However, the 0.2% proof strength better correlates with the stress at which hard deformation modes, such as {10.2} extension twinning and non-basal slip are activated. These modes are not as potently affected by the prismatic plate shaped precipitates. This finding helps to explain the modest age hardening response of Mg-Y-Nd-Zr alloys. Another strategy to greatly improve the age hardening response of Mg alloys is to increase the number density of particles, as proposed by Clark [2,3] some decades ago. Indeed, recent microalloying studies have demonstrated the potential to greatly improve the nucleation kinetics, precipitate number density, and hence, the age hardening response [e.g.2].

Acknowledgements

This research was sponsored by the Army Research Laboratory under Cooperative Agreement No. W911NF-07-2-0073, as a subcontract with Magnesium Elektron North America with Mr. Rick Delorme and Dr. Kyu Cho serving as Technical Contract Monitors. The views and conclusions contained in this document are those of the authors and should not be interpreted as representing the official policies, either expressed or implied, of the Army Research Laboratory or the U.S. Government. The U.S. Government is authorized to reproduce and distribute reprints for Government purposes notwithstanding any copyright notation hereon.

References

[1] Nie J.F. "Effects of precipitate shape and orientation on dispersion strengthening in magnesium alloys," Scripta Materialia, 48 (2003) 1009–1015.

[2] Clark J.B. “Age hardening in a Mg-9 wt.% Al alloy,” Acta Metallurgica, 16 (1968) 141-152.

[3] Clark J.B. “Transmission electron microscopy study of age hardening in a Mg-5 wt.% Zn alloy,” Acta Metallurgica, 13 (1965) 1281-1289.

[4] Nie J.F., Muddle B.C. “Precipitation in Magnesium Alloy WE54 during isothermal aging at 250°C,” Scripta Materialia, 40 (1999) 1089-1094.

[5] Agnew S.R., Tomé C.N., Brown D.W., et al. “Study of slip mechanisms in a magnesium alloy by neutron diffraction and modeling,” Scripta Materialia, 48 (2003) 1003–1008.

[6] Agnew S.R., Brown D.W., Tomé C.N. “Validating a Polycrystal Model for the Elasto-Plastic Response of Magnesium Alloy AZ31 Using In-situ Neutron Diffraction,” Acta Materialia, 54 (2006) 4841-4852.

[7] Muransky O., Barnett M.R., Carr D.G., Vogel S.C., Oliver E.C. “Investigation of deformation twinning in a fine-grained and coarse-grained ZM20 Mg alloy: Combined in situ neutron diffraction and acoustic emission,” Acta Materialia, 58, (2010) 1503-1517.

[8] Muransky O., Barnett M.R., Luzin V., et al. “On the correlation between deformation twinning and Luders-like deformation in an extruded Mg alloy: In situ neutron diffraction and EPSC.4 modelling,” Materials Science and Engineering A, 527 (2010) 1383-1394.

[9] Gharghouri M.A., Weatherly G.C., Embury J.D., Root J. “Study of the mechanical properties of Mg-7.7at.% Al by in situ neutron diffraction,” Philos. Magazine A, 79 (1999) 1671-1695.

[10] Jain J., Zou J., Poole W.J., Gharghouri M.A. “Reducing the tension-compression yield asymmetry in Mg-8Al-0.5Zn alloy via precipitation,” Scripta Materialia, 62 (2010) 301-304.

[11] Wu L., Jain A., Brown D.W., Stoica G.M., Agnew S.R., Clausen B., et al. “Internal stress relaxation and load redistribution during the twinning-detwinning-dominated cyclic deformation of a wrought magnesium alloy, ZK60A” Acta Materialia, 56 (2008) 3699-3707.

[12] Robson J. D., Stanford N., Barnett M. R., “Effect of particles in promoting twin nucleation in a Mg-5 wt.% Zn alloy,” Scripta Materialia, 63 (2010) 823-826.

[13] Robson J. D., Stanford N., Barnett M. R., “Effect of precipitate shape on slip and twinning in magnesium alloys,” Acta Materialia, 59 (2011) 1945–1956.

[14] Polesak J.P. “Constitutive behavior and microstructure evolution of magnesium alloy WE43 at temperatures and strain rates relevant to hot deformation processing,” (M.S. Thesis, University of Virginia, 2011).

[15] http://www.magnesium-elektron.com/data/downloads/DS467WE43.pdf.

[16] Bourke M.A.M., Dunand D.C., Üstündag E. “SMARTS - a spectrometer for strain measurements in engineering materials.” Applied Physics A, 74 [Suppl.] (2002) 3.

[17] Clausen, B., S.-Y. Lee, Üstündag E., et al. “Compressive yielding of tungsten fiber reinforced bulk metallic glass composites.” Scripta Materialia, 49 (2003) 6.

[18] Cáceres C., “Pseudoelastic behaviour of cast magnesium AZ91 alloy under cyclic loading–unloading,” Acta Materialia, 51 (2003) 6211-6218.

[19] Muransky O., Carr D. G., Sittner P., “In situ neutron diffraction investigation of deformation twinning and pseudoelastic-like behaviour of extruded AZ31 magnesium alloy,” International Journal of Plasticity, 25 (2009) 1107-1127.

[20] Stanford N. et al., “Effect of plate-shaped particle distributions on the deformation behaviour of magnesium alloy AZ91 in tension and compression,” Acta Materialia, 60 (2012) 218–228.

[21] Mendis C.L., Bettles C.J., Gibson M.A., Hutchinson C.R. “Enhanced age hardening response in Mg–Sn based alloys containing Zn,” Mater. Sci. Eng. A 435–436 (2006) 163–171.